Supplementary material for "Air-cushioning effect and Kelvin-Helmholtz instability before the slamming of a disc on water"

Utkarsh Jain,[1,*] Anaïs Gauthier,[1] Detlef Lohse,[1,2] and Devaraj van der Meer[1]

[1] *Physics of Fluids Group and Max Planck Center Twente for Complex Fluid Dynamics, MESA+ Institute and J. M. Burgers Centre for Fluid Dynamics, University of Twente, P.O. Box 217, 7500AE Enschede, The Netherlands*

[2] *Max Planck Institute for Dynamics and Self-Organization, Am Fassberg 17, 37077 Göttingen, Germany*

(Dated: April 20, 2021)

I. FLOW PROFILE IN THE THIN AIR GAP

An air flow is set up in the gap between the disc and water surface when it is squeezed out from the shrinking gap. For a thin gap d, we can ignore any azimuthal dependence of the air velocity and use the depth-integrated continuity equation:

$$\frac{\partial d}{\partial t} + \frac{1}{r}\frac{\partial}{\partial r}(r\, d\, V_{\text{air}}) = 0, \tag{1}$$

where V_{air} is the depth-averaged gas velocity in the gap and r is the radial coordinate centred on disc center. For a disc approaching at a velocity V, d can be substituted by $V(t_i - t)$, re-writing the above equation as

$$-V + \frac{1}{r}\frac{\partial}{\partial r}(rV(t_i - t)V_{\text{air}}) = 0. \tag{2}$$

Integrating and simplifying the above expression leads us to the expression for gas velocity

$$\mathbf{V}_{\text{air}} = \frac{r}{2}\frac{\hat{e}_r}{\tau}, \tag{3}$$

where we have replaced $(t_i - t)$ with τ, the amount of the time until the impact. Equation (3) is the same as the radial velocity in a squeeze layer [1, 2], and can alternately be derived by ignoring vertical velocities of the interstitial gas.

II. LINEAR KELVIN-HELMHOLTZ ANALYSIS FOR SHALLOW AIR LAYER

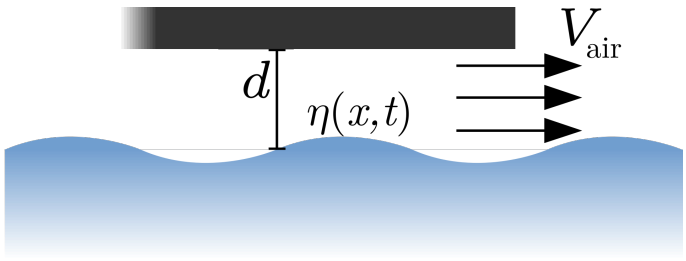

FIG. S1. Schematic outlining some parameters in the present Kelvin-Helmholtz problem.

Our problem consists of an initially stationary water surface located at $z = 0$, over which air flows with a presumed constant velocity V_{air} in a finite, confined gap of width d. In two dimensions, let the interface deformation be denoted by

$$z = \eta(x, t). \tag{4}$$

* u.jain@utwente.nl

Here z is the vertical coordinate, x the horizontal, and t the time. For an inviscid flow, whose potential is denoted by $\phi(x, z, t)$, the usual condition holds for incompressibility:

$$\nabla^2 \phi^i = 0, \tag{5}$$

while the equations of motion yield the unsteady Bernoulli in each phase equation

$$\frac{p^{\mathrm{i}}}{\rho^i} + \frac{1}{2}(\nabla\phi^i)^2 + gz + \frac{\partial \phi^i}{\partial t} = f^i(t), \tag{6}$$

where i is used in place of specifying air and water. Acceleration due to gravity is denoted by g. The following conditions hold at the interface $z = \eta(x, t)$:

$$\frac{\partial \eta}{\partial t} - \frac{\partial \phi^i}{\partial z} + (\nabla\phi^i).(\nabla\eta) = 0, \tag{7}$$

and

$$p^{\mathrm{air}} - p^{\mathrm{water}} = \sigma\kappa, \tag{8}$$

where σ and κ respectively are the surface tension and curvature of the interface. In the water pool,

$$\frac{\partial \phi^{\mathrm{water}}}{\partial z} = 0 \text{ as } z \to -\infty. \tag{9}$$

while in air,

$$\frac{\partial \phi^{\mathrm{air}}}{\partial z} = 0 \text{ at } z = d. \tag{10}$$

To analyse the system's stability, we introduce small perturbations to the state variables η, ϕ and p as

$$\eta = \eta_0 + \eta_1,\ \phi^i = \phi_0^i + \phi_1^i \text{ and } p^i = p_0^i + p_1^i, \tag{11}$$

with $\eta_0 = 0$, $\phi_0^{\mathrm{water}} = 0$, $\phi_0^{\mathrm{air}} = V_{\mathrm{air}}\, x$. Pressures p_0^i are the respective hydrostatic pressures. We retain the presumably small perturbation terms only upto first order. We find the following equations governing the flow and behaviour at the interface [3]

$$\nabla^2 \phi_1^{\mathrm{water}} = 0, \qquad -\infty < z < 0, \tag{12}$$

$$\nabla^2 \phi_1^{\mathrm{air}} = 0, \qquad 0 < z < d, \tag{13}$$

$$\frac{\partial \eta_1}{\partial t} - \frac{\partial \phi_1^{\mathrm{water}}}{\partial z} = 0, \qquad \text{at } z = 0^-, \tag{14}$$

$$\frac{\partial \eta_1}{\partial t} - \frac{\partial \phi_1^{\mathrm{air}}}{\partial z} + V_{\mathrm{air}}\frac{\partial \eta_1}{\partial x} = 0, \qquad \text{at } z = 0^+, \tag{15}$$

$$\rho^{\mathrm{water}}\left(g\eta_1 + \frac{\partial \phi_1^{\mathrm{water}}}{\partial t}\right) - \rho^{\mathrm{air}}\left(g\eta_1 + \frac{\partial \phi_1^{\mathrm{air}}}{\partial t} + V_{\mathrm{air}}\frac{\partial \phi_1^{\mathrm{air}}}{\partial x}\right) = \sigma\left(\frac{\partial^2 \eta_1}{\partial x^2}\right), \qquad \text{at } z = 0, \tag{16}$$

$$\frac{\partial \phi_1^{\mathrm{water}}}{\partial z} = 0, \qquad \text{as } z \to -\infty, \tag{17}$$

$$\frac{\partial \phi_1^{\mathrm{air}}}{\partial z} = 0 \qquad \text{at } z = d. \tag{18}$$

Equations (14), (15) are the kinematic boundary conditions while equation (16) is the dynamic boundary condition at the interface η_1. Following [3, 4], we consider the following form of perturbations:

$$\eta_1 = A \exp i(kx - \omega t), \tag{19}$$

$$\phi_1^{\mathrm{water}} = B \exp(kz) \exp i(kx - \omega t), \text{ and} \tag{20}$$

$$\phi_1^{\mathrm{air}} = C \cosh k(z - d) \exp i(kx - \omega t), \tag{21}$$

where A, B and C are amplitudes of supposed perturbations, k the wavenumber and ω the complex temporal growth rate of perturbations. They are chosen such that that the $z-$dependent parts of ϕ_1^{water} and ϕ_1^{air} satisfy the Laplace equation and the far-field conditions in their respective half-spaces, as specified by equations (17)–(18). Substituting equations (19)–(21) into equations (14)–(16) leads to

$$-i\omega A - kB = 0, \tag{22}$$

$$-i\omega A + kC\sinh(dk) + V_{\text{air}} \cdot ikA = 0, \text{ and} \tag{23}$$

$$\rho^{\text{water}}(gA - iB\omega) - \rho^{\text{air}}\Big(gA - i\omega C\cosh(kd) + V_{\text{air}} \cdot Cik\cosh(kd)\Big) = \sigma A(ik)^2. \tag{24}$$

The above equations can be solved to obtain a quadratic equation for ω, which yields the dispersion relation of the form

$$\omega_{\pm}(k) = \Xi \pm \sqrt{\Delta}\,, \tag{25}$$

where the discriminant Δ is

$$\Delta = \frac{k^3\sigma}{\rho^{\text{water}} + \rho^{\text{air}}T} - \frac{k^2\rho^{\text{water}}\rho^{\text{air}}TV_{\text{air}}^2}{(\rho^{\text{water}} + \rho^{\text{air}}T)^2} + \frac{k(\rho^{\text{water}} - \rho^{\text{air}})}{\rho^{\text{water}} + \rho^{\text{air}}T}\,, \tag{26}$$

wherein $T = \coth(dk)$. The temporal growth rate of instability is given by $\mathcal{I}m[\omega_+(k)]$, which occurs when $\Delta < 0$. The minimum velocity of air $V_{\text{air}}^{\min}$ for instability to grow can be found from the condition $\Delta = 0$ as

$$V_{\text{air}}^{\min} = \frac{\sqrt{(g\rho^{\text{water}} - g\rho^{\text{air}} + \sigma k^2)(\rho^{\text{water}} + \rho^{\text{air}}T)}}{\sqrt{k\rho^{\text{water}}\rho^{\text{air}}T}}. \tag{27}$$

The instability is expected to occur for all $V_{\text{air}} \geq V_{\text{air}}^{\min}$.

From equation (3), the velocity of escaping air is highest at the disc edge at $r = D/2$, which corresponds to the region where the instability is seen to grow. It is seen that $V_{\text{air}}^{\min}$ depends primarily on the properties of the two fluids and their interface, which is to be expected in such an interfacial instability. However, an additional dependence on the thickness of the air layer d is contained in the term T via $\coth(dk)$, where the classical result is derived for $T = 1$ (i.e., $dk \gg 1$). Finally, a numerical value for $V_{\text{air}}^{\min}$ can be found if the values of maximal unstable wavenumber and d at the onset of instability are known. To find the former, we can determine the marginally unstable solution, which is discussed henceforth.

Stability curves in (d, k) space are found by substituting equation (27) into the expression for Δ (equation (26)). It is then seen that $\Delta(k)$ has a maximum. The marginally stable wavenumber, namely that wavenumber at which the solution first becomes unstable, k^{marg}, is then found by finding the maxima of $\Delta(k)$ at $V_{\text{air}} = V_{\text{air}}^{\min}$. For a fixed pair of fluids (here, air-water), the only parameter to remain variable from our calculations is the thickness of air layer, d. At the point of marginal stability, the air layer thickness is $d = d^{\text{marg}}$. In figure S2, we plot the derivative of expression in (26), $\Delta'(k)$, for some values of d^{marg}, keeping the physical parameters for the water-air interface for some values of d^{marg} from our experiments (figure 3, main manuscript). We find that the most unstable wavenumber corresponding to $\Delta'(k) = 0$ is usually approximately 368 1/m, which corresponds to a marginally unstable wavelength $\lambda^{\text{marg}} \approx 1.7$ cm. Any modification to this result, originating from a finite thickness of the air layer, is contained via the term T in our solution. From figure S2, it can be seen that the marginally unstable wavelength starts to deviate from the set of solutions without the effect of term T as d decreases past approximately 8 mm.

Thus we may use $k^{\text{marg}} = 368$ m^{-1} to estimate $V_{\text{air}}^{\min}$ at the air water interface, leaving d^{marg} as a variable parameter. The dependence of $V_{\text{air}}^{\min}$ on air-layer thickness at the onset of instability is still contained via the term T, and can be computed as shown in figure S3.

An alternate way to directly correlate d^{marg} and λ^{marg} is to numerically find the unique solutions to the expressions that are satisfied at marginal stability:

$$\Delta(k) = 0, \text{ and} \tag{28}$$

$$\Delta'(k) = 0. \tag{29}$$

The results are plotted in figure S4. We find that in our system, the most unstable wavelength at the onset of instability is only affected by finiteness of the air-layer when $d^{\text{marg}} \lesssim 7$ mm. For any greater d^{marg}, λ^{marg} rapidly converges to approximately 1.7 cm, which is the classical solution found in the absence of finite-layer effects in air.

[1] S. Ishizawa, Bulletin of JSME **9**, 533 (1966).

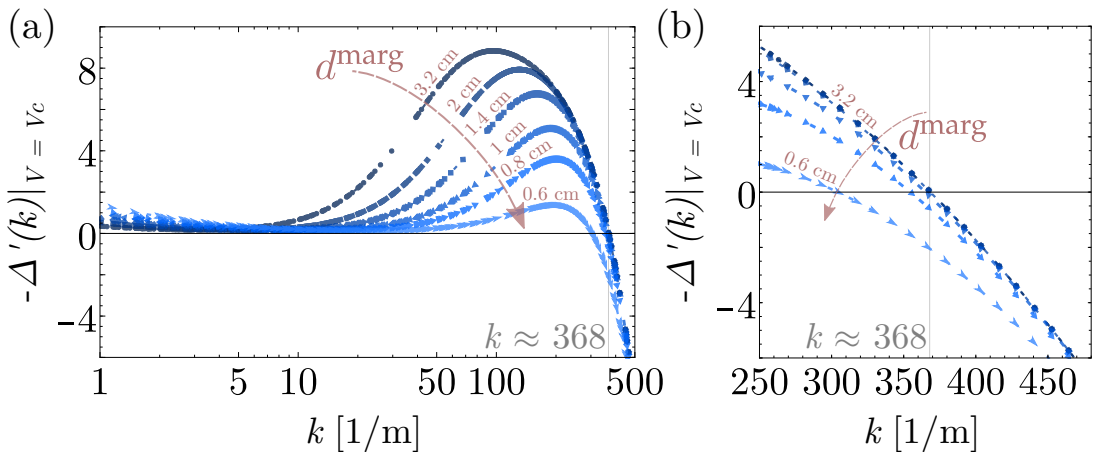

FIG. S2. (a) The derivative $\Delta'(k)$ from equation (26) is plotted as a function of k for various values of the measured air layer thickness at instability onset d^{marg}.The marginally unstable wavenumber is found at $k^{\mathrm{marg}} \approx 368$ m^{-1} for relatively thick air-layers, a value which is typically found from Kelvin-Helmholtz instability analysis at air-water interface when both the fluid phases are infinitely deep. k^{marg} starts to vary substantially from the asymptotic found result only for increasingly thinner air-layers of the order of a few millimeters. Panel (b) contains the same results as panel (a), only now focusing in the region $k \in [250, 480]$, as the marginally unstable wavelength lies in this region.

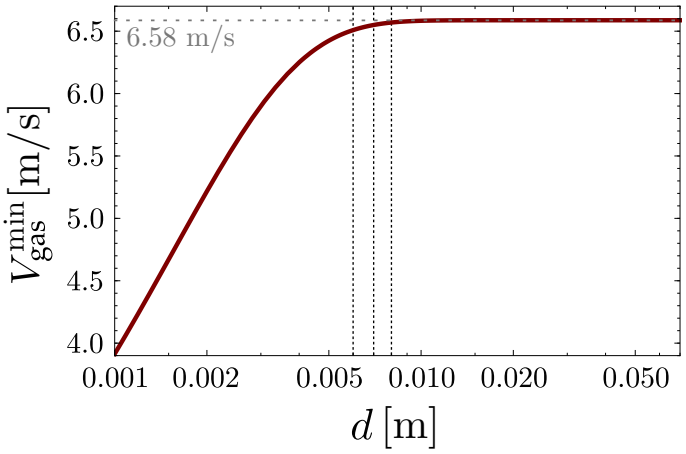

FIG. S3. Variation of $V_{\mathrm{air}}^{\mathrm{min}}$ with d^{marg} for air-water interface. We see that finite-thickness effects due to the shallow air layer only start to affect the solutions when is of the order of a few millimetres. Calculations for $V_{\mathrm{air}}^{\mathrm{min}}$ at $k^{\mathrm{marg}} = 368$ m^{-1} rapidly asymptote to those derived for semi-infinite media separated by air-water interface. Black dashed lines highlight the gap widths $d = 6$, 7 and 8 mm.

[2] J. Jackson, Applied Scientific Research, Section A volume **11**, 148 (1963).
[3] D.-Y. Hsieh and S. Ho, *Wave and Stability in Fluids* (World Scientific, 1994).
[4] S. Chandrasekhar, *Hydrodynamic and Hydromagnetic Stability*, Dover Books on Physics Series (Dover Publications, 1981).

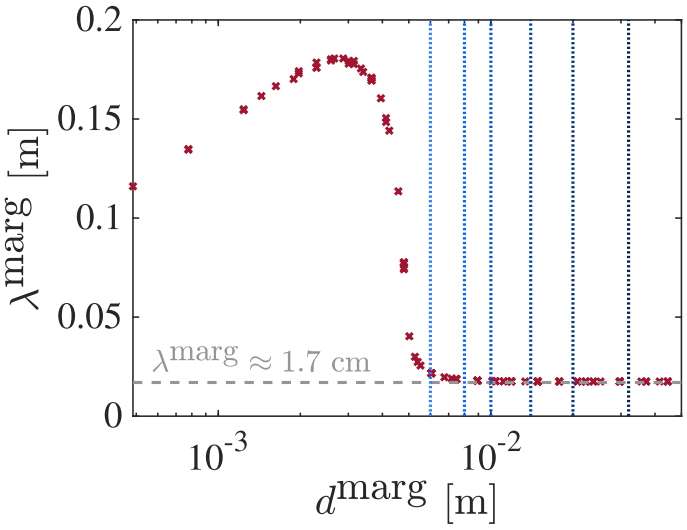

FIG. S4. Numerical solutions to the marginal stability criteria (equations (28) and (29)) plotted in terms of λ^{marg} vs d^{marg}. The dotted lines are colour-coded the same as in figure S2 to highlight where d^{marg} used to calculate marginal stability curves in figure S2 lie here.